JOURNAL OF VIROLOGY, July 1998, p. 5343–5350 Vol. 72, No. 7
0022-538X/98/$04.00+0

The Latent Herpes Simplex Virus Type 1 Genome Copy Number in Individual Neurons Is Virus Strain Specific and Correlates with Reactivation

N. M. SAWTELL,[1] D. K. POON,[2] C. S. TANSKY,[1] AND R. L. THOMPSON[2]*

Division of Infectious Diseases, Children's Hospital Medical Center, Cincinnati, Ohio 45229-3039,[1] and Department of Molecular Genetics, Microbiology, and Biochemistry, University of Cincinnati Medical Center, Cincinnati, Ohio 45267-0524[2]

Received 10 December 1997/Accepted 12 March 1998

The viral genetic elements that determine the in vivo reactivation efficiencies of fully replication competent wild-type herpes simplex virus (HSV) strains have not been identified. Among the common laboratory strains, KOS reactivates in vivo at a lower efficiency than either strain 17syn+ or strain McKrae. An important first step in understanding the molecular basis for this observation is to distinguish between viral genetic factors that regulate the establishment of latency from those that directly regulate reactivation. Reported here are experiments performed to determine whether the reduced reactivation of KOS was associated with a reduced ability to establish or maintain latent infections. For comparative purposes, latent infections were quantified by (i) quantitative PCR on DNA extracted from whole ganglia, (ii) the number of latency-associated transcript (LAT) promoter-positive neurons, using KOS and 17syn+ LAT promoter–β-galactosidase reporter mutants, and (iii) contextual analysis of DNA. Mice latently infected with 17syn+-based strains contained more HSV type 1 (HSV-1) DNA in their ganglia than those infected with KOS strains, but this difference was not statistically significant. The number of latently infected neurons also did not differ significantly between ganglia latently infected with either the low- or high-reactivator strains. In addition to the number of latent sites, the number of viral genome copies within the individual latently infected neurons has recently been demonstrated to be variable. Interestingly, neurons latently infected with KOS contained significantly fewer viral genome copies than those infected with either 17syn+ or McKrae. Thus, the HSV-1 genome copy number profile is viral strain specific and positively correlates with the ability to reactivate in vivo. This is the first demonstration that the number of HSV genome copies within individual latently infected neurons is regulated by viral genetic factors. These findings suggest that the latent genome copy number may be an important parameter for subsequent induced reactivation in vivo.

The capacity of latent herpes simplex virus (HSV) to reactivate is essential for completion of the viral life cycle. Reactivation is thus an important target for intervention to prevent not only recurrent disease but also spread through the population. Current molecular level understanding of events controlling reactivation is minimal. It is clear that mutations that result in reduced viral replication efficiency in all cell types have a negative impact on both the establishment of latency and the ability to reactivate (2, 12, 16, 35). Mutations that result in replication deficits in nondividing cells, such as thymidine kinase (TK)-negative mutants, also result in reactivation defects (10, 13, 14, 36). Mutations within the 5′ end or promoter region of the latency-associated transcript (LAT) gene do not affect viral replication in any cell type but result in reduced reactivation in vivo in rabbits and mice (1, 8, 9, 18, 31, 38). In the murine model, it has been demonstrated that LAT mutants establish significantly fewer latent infections, and this most likely accounts for the reduction in reactivation observed (31, 38). Whether this is also the case for LAT mutants in the rabbit model awaits analysis of establishment at the cellular level in this species. Among the commonly used fully replication competent wild-type HSV type 1 (HSV-1) laboratory strains, KOS differs significantly from strains 17syn+ and McKrae in the capacity to reactivate from latency when induced in vivo (1, 8, 9, 24, 29, 34). In contrast, the recovery of infectious virus by in vitro cocultivation from ganglia latently infected with these strains is not different, suggesting that additional barriers must be overcome for efficient induced viral reactivation in vivo. The viral genetic factors that account for the difference in replication-competent strains to reactivate in vivo have not been identified (34).

There are two distinct but not mutually exclusive alternatives: (i) KOS/M is less efficient in the establishment of latent infections, or (ii) KOS/M is less efficient directly in in vivo reactivation. While it is clear that latent infections are required for reactivation, the characteristics of latent infections that predispose to reactivation have not yet been defined. A positive correlation between the amount of total latent DNA in the ganglia and the ability to recover infectious virus from the latently infected ganglia by cocultivation in mice has been reported (12, 16, 31). In the mouse and rabbit ocular models, the number of neurons positive for LAT RNAs by in situ hybridization was positively correlated with frequency or timing of reactivation (6, 18, 35). The same was true for activity from the LAT promoter in the mouse (31). Using a recently developed assay, contextual analysis of DNA (CXA-D), to measure latent infections on the single-cell level, we have shown that increasing inoculum titer results in more neurons

* Corresponding author. Mailing address: University of Cincinnati Medical Center, Department of Molecular Genetics, Microbiology, and Biochemistry, 231 Bethesda Ave., Cincinnati, OH 45267-0524. Phone: (513) 558-0063. Fax: (513) 558-8474. E-mail: Richard.Thompson@UC.edu.

† Present address: NCI-Frederick Cancer Research and Development Center, Frederick, MD 21702-1201.

harboring latent viral genomes, with a greater number of genomes per latently infected neuron (28). In another study, increasing the number of latently infected neurons in the ganglia resulted in an increased frequency of reactivation (38).

An important first step in understanding the molecular basis for the difference between in vivo reactivation of fully replication competent strains is to distinguish between viral genetic factors that regulate the establishment of latency from those that directly regulate reactivation. In this study, a comprehensive analysis of the establishment of latency of strains 17syn+ and KOS/M determined not only the number of latently infected neurons within the ganglia but also the number of viral genome copies contained in individual latently infected neurons. For comparative purposes, latency was quantified by quantitative PCR (QPCR) on DNA extracted from whole ganglia, assessment of the number of LAT-expressing neurons by using LAT promoter-reporter mutants, and determination of the percentage of viral genome-positive neurons by using CXA-D. The number of latently infected neurons was not different in KOS/M-, 17syn+-, or McKrae-infected ganglia. Although QPCR revealed no significant difference in the total amount of viral DNA in KOS/M- compared to 17syn+-infected ganglia, when analyzed at the single-cell level, neurons latently infected with strain KOS/M contained significantly fewer viral genome copies compared to those infected with either strain 17syn+ or strain McKrae. This is the first demonstration that there is a strain-dependent variation in the latent viral genome copy number profile, establishing that viral genetic factors regulate the number of viral genome copies present within latently infected neurons. The fact that the latent pools generated by the efficient reactivator strains were similar, and both contained a greater number of viral genome copies than the KOS/M latent pool, suggests that copy number influences the efficiency of induced in vivo reactivation.

MATERIALS AND METHODS

Cell and virus culture. Rabbit skin cells were cultured as previously described (39). NIH 3T3 cells were obtained from the American Type Culture Collection (CRL 6442) and were cultured as recommended. Virus strains used were derived from wild-type (wt) HSV-1 strain 17syn+, obtained from J. Subak-Sharpe of the Medical Research Council Virology Unit in Glasgow, Scotland; strain KOS, obtained from M. Levine, University of Michigan, Ann Arbor, was plaque purified and designated KOS/M; strain McKrae was obtained from S. Wechsler, Mount Cedar Sinai Medical Center Research Institute. The derivations and histories of these viruses have been previously described (24, 38).

Construction of viral mutants. KOS/1 (kindly provided by L. T. Feldman) was constructed from the parental strain KOS/M and has been described previously (19, 31). Briefly, approximately 850 bp of the LAT promoter was placed in front of the *Escherichia coli* β-galactosidase (β-Gal) gene and inserted into the *Eco*RV site within the glycoprotein C (gC) locus at bp 97646. This resulted in the disruption of gC and the expression of β-Gal during latency. 17/1, derived from the parental strain 17syn+, was constructed to be exactly like KOS/1. To facilitate this, the fragment that contains the gC locus (*Bgl*II-G) was cloned from KOS/1 into pSP73 (Promega, Madison, Wis.) at the *Bgl*II site. This fragment was recombined into the 17syn+ genome by cotransfection with LipofectACE (GIBCO/Bethesda Research Laboratories, Gaithersburg, Md.) according to the manufacturer's protocol. The 17syn+-based LAT promoter–β-Gal reporter virus (designated 17/1) was plaque purified to homogeneity by limiting dilution. The genomic structure of 17/1 was confirmed by restriction fragment length polymorphism (RFLP) Southern blot analysis as previously described (31, 37, 38, 40) and is shown schematically in Fig. 1A. Base pair numbering is as published for the HSV-1 sequence of strain 17syn+ (20–22 [GenBank accession no. 14112]).

Inoculation of mice. Male Swiss Webster mice weighing 18 to 22 g were obtained from Charles River Breeding Laboratories (Kingston, N.Y.) or Harlan Laboratories (Indianapolis, Ind.). Animals were housed in American Association for Laboratory Animal Care-approved quarters with unlimited access to food and water. Mice were anesthetized by intraperitoneal injection of sodium pentobarbital at a dose of 50 mg/kg of body weight. Anesthetized mice were inoculated by placing 1×10^5 to 2×10^5 PFU of virus onto the surface of scarified corneas as described previously (29, 31). In certain experiments bilateral 5-mm areas on the whisker pad were also inoculated as described previously (31). In these cases, mice received a total of 3×10^5 PFU.

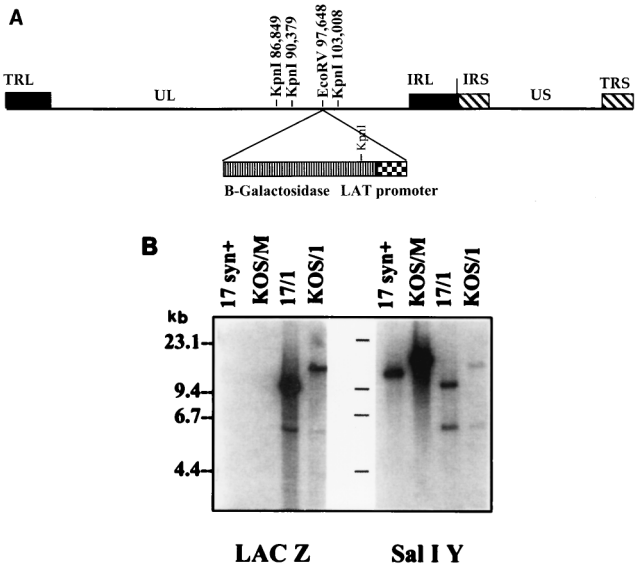

FIG. 1. (A) Schematic of the HSV-1 genome. The terminal repeat long, unique long, internal repeat long, internal repeat short, unique short, and terminal repeat short portions of the genome are labeled TRL, UL, IRL, IRS, US, and TRS, respectively. Relevant *Kpn*I restriction endonuclease sites and the location of the LAT promoter–β-Gal insert are indicated. (B) Viral DNAs were cleaved with *Kpn*I, electrophoresed, blotted, and probed as described in Materials and Methods. Left, probe is a 624-bp *Hpa*I fragment from the *lacZ* gene present in plasmid pCH110; right, probe is HSV-1 *Sal*I fragment Y (bp 94853 to 98422 on the viral genome [19]).

Replication kinetics. Multistep replication kinetic analyses were performed on NIH 3T3 monolayers following infection at a low multiplicity of infection (0.01 PFU/cell). Cells and media were harvested at the indicated times, subjected to three cycles of freezing and thawing, and assayed for infectious virus titer on rabbit skin cell monolayers.

Mice were inoculated as described above. At the indicated times postinfection (p.i.), mice were sacrificed, the appropriate tissues were removed and homogenized, and virus titers were determined as described above.

Induced reactivation in vivo. Latently infected mice were subjected to the transient hyperthermia induction procedure described previously (29). Briefly, mice which had been inoculated a minimum of 30 days prior were subjected to a 10-min hyperthermic stress (43°C); 22 h posttreatment trigeminal ganglia (TG) were removed and assayed for infectious virus. DNA was harvested from positive cultures and analyzed for RFLP by Southern blotting to confirm the genomic structure of the isolate as described elsewhere (reference 38 and data not shown).

QPCR of HSV DNA in latently infected ganglia. QPCR was carried out precisely as described previously (12, 28, 31, 38). The resulting blots were scanned in a Molecular Dynamics PhosphorImager for quantification using ImageQuant software (Molecular Dynamics).

Histochemical detection of β-Gal activity. Mice were inoculated with 17/1 or KOS/1 as described above. On days 7, 15, and 30 p.i., animals were anesthetized and perfused; the ganglia were harvested and incubated in 5-bromo-4-chloro-3-indolyl-β-D-galactopyranoside (X-Gal) buffer containing 0.1 μg of X-Gal per ml as described previously (31). The number of neurons containing the blue X-Gal product was determined in a double-blind fashion.

Immunohistochemical detection of HSV antigen in combination with histochemical detection of β-Gal activity. Mice were inoculated with 17/1 or KOS/1 as described above. On days 4 and 7 p.i., three animals from each inoculation group were anesthetized and perfused with 4% paraformaldehyde; the TG were harvested and incubated at 37°C in X-Gal buffer containing 0.1 μg of X-Gal (Gibco-BRL) per ml for 12 h. Ganglia were rinsed in phosphate-buffered saline (PBS), postfixed in 4% paraformaldehyde for 15 min, dehydrated through graded ethanols, cleared in xylene, and embedded in paraffin (six ganglia per block) according to routine procedures. Blocks were sectioned at 8 μm; sections were placed on glass slides (Superfrost Plus; Sigma) and baked at 60°C for 12 h. Paraffin was removed in xylene, sections were rehydrated in graded ethanols, and endogenous peroxidase activity was removed by incubating sections in methanol containing 0.75% H_2O_2 for 15 min. Sections were rinsed in PBS and placed in PBS containing 5% nonfat dry milk and 0.25% Nonidet P-40 for 30 min. To localize HSV antigens, antiserum raised in rabbits against HSV (Accurate) diluted 1:1,500 was used in a standard three-step biotin-avidin-horseradish peroxidase assay (31). The secondary antibody used was a biotinylated anti-rabbit

immunoglobulin G raised in goat (Vector), and the conjugate was an avidin-horseradish peroxidase made and purified as described previously (29). Antigen antibody complexes were visualized by incubating sections in a solution of 0.1 M Tris (pH 8.2) containing 250 μg of diaminobenzidine (Sigma) per ml and 0.004% H_2O_2. Stained sections were viewed and photographed with an Olympus model BX40 photomicroscope.

CXA-D. The details of the CXA-D procedure have been reported previously (28). In brief, deeply anesthetized mice were perfusion fixed with Streck's tissue fixative (STF) (Streck Laboratories, Inc.). The tissues of interest were removed, finely minced, and placed in a solution of 0.25% collagenase (CLS I; Worthington) in Hanks balanced salt solution at 37°C. At completion, the dissociated tissue was gently pelleted, the collagenase was removed, and the pellet was resuspended in STF for a 15-min postfixation. Enriched neuronal cell populations were obtained by using Percoll gradient centrifugation as described previously (28).

PCR analysis of DNA within perfusion-fixed dissociated cells. Dissociated, gradient-purified neurons were rinsed in distilled H_2O. A portion of the cells was diluted so that the desired number to be analyzed was contained in a 1-μl volume. To allow visualization of the cells, Ponceau S solution was added (1/200 volume), the cells were then aliquoted into PCR tubes, and the exact number was determined by counting under a dissecting microscope. To remove any extracellular contaminating DNA, immobilized DNase on polyvinylpyrrolidone beads (Mobitec) was added to each sample as described previously (28). Following overnight incubation at 37°C, the DNase was heat inactivated and samples were incubated at 50°C in a proteinase K solution for 3 h. PCR amplification using primers to the viral TK gene was performed as previously described (12, 28, 31, 38). Five microliters of each PCR product was electrophoresed through a 12% polyacrylamide gel, transferred to a nylon membrane (GeneScreen Plus), and probed with a ^{32}P end-labeled oligonucleotide internal to the PCR primers as described previously (12, 31). The blots were exposed to a storage PhosphorImager cassette (Molecular Dynamics) and analyzed according to the manufacturer's protocol, using ImageQuant software.

Statistical analysis. Statistical analysis of the data was performed with Prism version 2.0 software (GraphPad).

RESULTS

Construction and characterization of 17/1 and KOS/1. Promoter-reporter mutants in the two strains were constructed as described above. The genomic structures of the resulting mutants 17/1 and KOS/1 are shown schematically in Fig. 1A. These structures were confirmed by Southern blot RFLP analysis as previously described (31, 37, 38, 40). Representative blots are shown in Fig. 1B. The viral DNAs were cleaved with *Kpn*I and probed sequentially with radiolabeled sequences specific for the *E. coli* β-Gal gene and the HSV *Sal*I Y fragment. As expected, no hybridization was seen in the 17syn+ and KOS/M lanes when probed with β-Gal. The 17/1 lane shows two hybridizing bands of 9.4 and 6.1 kb, and the KOS/1 lane shows two bands of 13 and 6.1 kb, which are in agreement with the predicted sizes. KOS/M is missing the *Kpn*I site at bp 90379 (37), and thus the larger fragment is the result of cleavage at the next site to the left at bp 86849. When probed with the *Sal*I Y fragment, lanes containing wt viral DNAs show bands of 12.7 and 16 kb for 17syn+ and KOS/M, respectively. The β-Gal virus lanes show bands of 9.4 and 6.1 kb for 17/1 and bands of 13 and 6.1 kb for KOS/1, which are also in agreement with the predicted sizes. Further restriction endonuclease and Southern blot analyses did not reveal any unexpected perturbations in the genomes (data not shown).

Acute replication kinetics. Multistep replication kinetics in cultured cells confirmed that no general replication defect was present in any of the viruses (Fig. 2). In vivo, all viruses reached a peak titer by 4 days p.i. Eyes, snouts, and TG were analyzed for infectious virus at 24-h intervals after inoculation (Fig. 2). The peak titers of 17/1 and KOS/1 were twofold less than those for the parental strains in all tissues tested. The reason for this has not been determined but may be due to the loss of gC, which has been shown to augment binding and entry (7). In vivo replication kinetics assays were also performed on mice from the groups that were subsequently analyzed using CXA-D. For these experiments, mice were inoculated on scarified corneal surfaces, and eyes and TG were harvested from

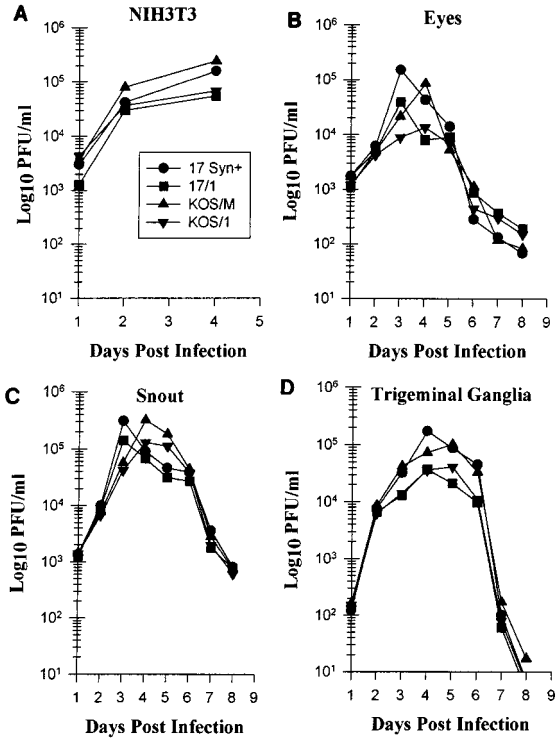

FIG. 2. (A) NIH 3T3 cells were infected at a low multiplicity (0.001 PFU/cell). At 24-h intervals, triplicate cultures were assayed for virus content. (B to D) Mice were infected with a total of 3×10^5 PFU of the virus isolates on the corneas and snouts as described in Materials and Methods. At daily intervals, three mice from each group were sacrificed, and the eyes, snouts, and TG were homogenized and assayed for infectious virus.

three mice/group on days 2, 4, 6, and 8 p.i. Consistent with other experiments, the infectious titers achieved by KOS/M, 17syn+, and McKrae in both the eyes and TG were equivalent (data not shown).

Induced reactivation of 17syn+, 17/1, KOS/M, and KOS/1 in TG. The hyperthermia model of induced reactivation (29) was used to examine the ability of the selected HSV-1 strains to reactivate in vivo. The results from this experiment are presented in Table 1. The frequencies of reactivation for the wt viruses in this study (86% for 17syn+ and 30% for KOS/M [$P = 0.001$, Fisher's exact test]) were consistent with a previous report (29). The difference in reactivation frequency was also displayed by the promoter-reporter mutants (83% for 17/1 and 15% for KOS/1; $P = 0.001$). The frequency of reactivation following hyperthermic stress was also determined for mice in

TABLE 1. Efficiency of in vivo reactivation following hyperthemic stress[a]

Virus	No. of mice positive/no. tested (% reactivation)	
	Expt 1	Expt 2
17syn+	12/14 (86)	7/10 (70)
KOS/M	10/33 (30)	4/20 (20)
17/1	10/12 (83)	ND
KOS/1	2/13 (15)	ND

[a] Mice were infected as described in the text and maintained for at least 30 days prior to being subjected to the hyperthermic stress reactivation procedure as described previously (30). ND, not determined.

TABLE 2. Quantification of latent viral genomes, using whole-ganglion QPCR[a]

Virus	No. of TG pairs	No. of genomes/TG pair	
		Mean ± SD	Range
17syn+	12	$2.0 \times 10^5 \pm 1.3 \times 10^5$	2.3×10^4–4.9×10^5
KOS/M	12	$1.2 \times 10^5 \pm 7.5 \times 10^4$	3.4×10^4–3.1×10^5
17/1	10	$5.2 \times 10^4 \pm 3.2 \times 10^4$	3.3×10^3–4.3×10^5
KOS/1	10	$4.1 \times 10^4 \pm 3.0 \times 10^4$	2.6×10^3–1.7×10^5

[a] QPCR was performed at 30 days p.i. on DNA extracted from pairs of latently infected TG as described previously (12, 31).

the groups to be analyzed by CXA-D. These mice, inoculated via corneal scarification, also exhibited a difference in reactivation, 7 of 10 (70%) 17syn+-infected mice, compared to 4 of 20 (20%) of the KOS/M-infected group ($P = 0.01$).

Analysis of HSV DNA present in latently infected TG by QPCR. The QPCR method of Katz et al. (12) was used to determine the number of latent viral genomes present in whole ganglia (Table 2). The amount of viral DNA present in each pair of latently infected TG was variable, consistent with previous studies using this method (12, 31, 38). A comparison of the mean genome copy number per animal and a one-way analysis of variance did not reveal any statistically significant differences between any of the viruses. Therefore, by this criterion, KOS/M and KOS/1 established latency as well as 17syn+ and 17/1.

Characterization of cell type and HSV antigen expression in LAT promoter-positive TG cells on days 4 and 7 p.i. Our previous in vivo analysis of KOS/1 revealed three important points with respect to LAT promoter–β-Gal reporter activity: (i) activity in the TG peaked during the acute infection between days 4 and 5; (ii) activity localized to neurons, so designated on the basis of location, size, and morphology; and (iii) the vast majority of β-Gal-expressing neurons showed no evidence of viral protein production and thus were considered to be neurons entering latency (31). Additional studies using an antibody to a neuron-specific marker (neurofilament 200) confirmed that our assessment of neurons based on morphology was correct (data not shown). Similar findings with the basal LAT promoter have been reported by others (19). To confirm that mutant 17/1 behaved in a similar manner, mice were infected with KOS/1 and 17/1 as described in Materials and Methods. The type of cell expressing β-Gal and the extent of lytic viral protein expression in the β-Gal-expressing cells were determined on days 4 and 7 p.i. 17/1 and KOS/1 were indistinguishable with respect to (i) the restriction of expression of β-Gal to neurons in the TG and (ii) the absence of detectable HSV lytic protein expression in the vast majority of neurons expressing β-Gal (Fig. 3). There were many HSV antigen-positive neurons and support cells in both KOS/1- and 17/1-infected TG on day 4. Thus, the blue neurons appear to mark

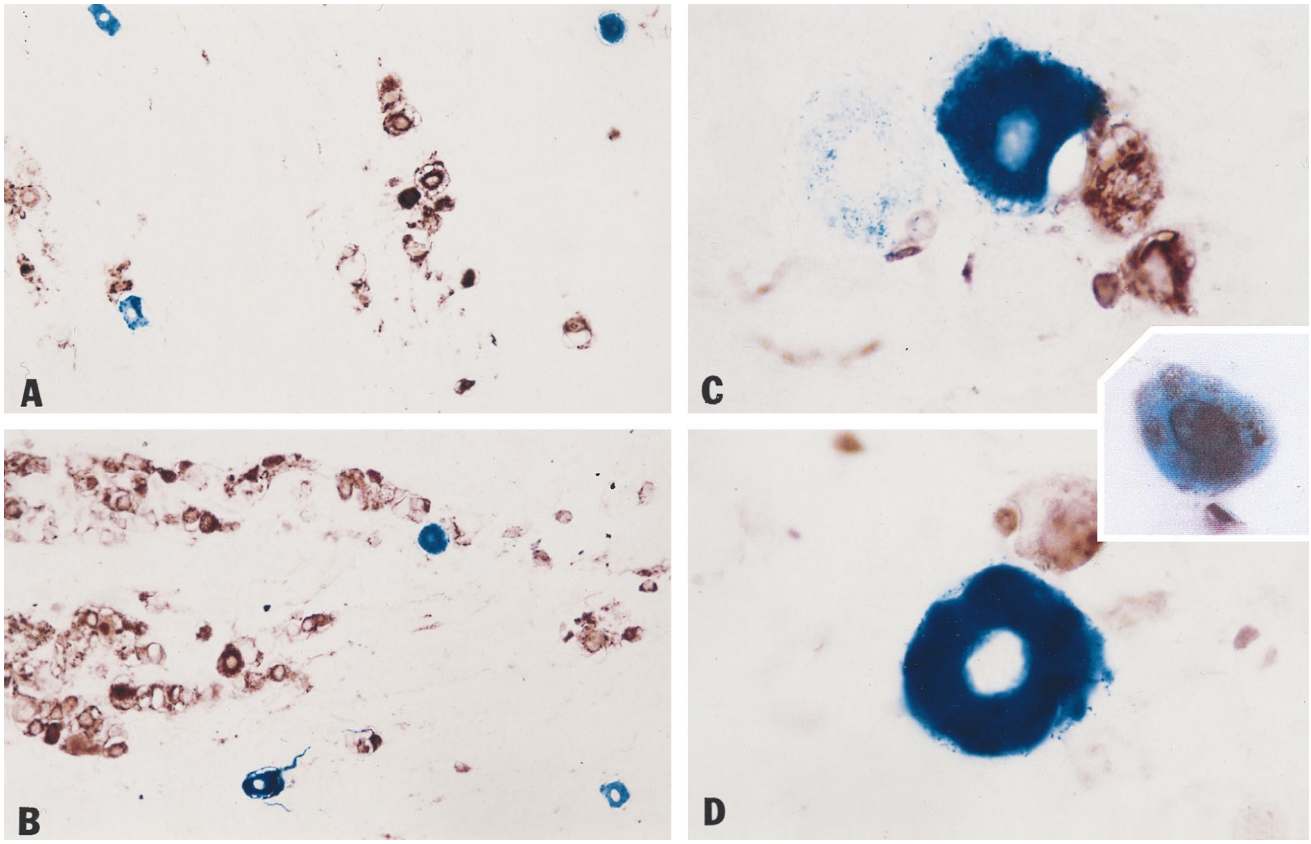

FIG. 3. Dual localization of HSV antigen and LAT promoter activity in TG during acute infection with 17/1 and KOS/1 (photomicrograph of sectioned TG on day 4). Both 17/1 (A)- and KOS/1 (C)-infected ganglia contain many HSV antigen-positive neurons and support cells. The fields shown were selected because several β-Gal-containing neurons were present. The difference in the number of antigen-positive cells in the 17/1 and KOS/1 sections shown is not representative. The vast majority (>90%) of β-Gal-expressing neurons were devoid of detectable HSV antigen in both 17/1 (B)- and KOS/1 (D)-infected ganglia. However, with both, there were a few neurons in which HSV antigen could be detected (inset). In agreement with previous findings, β-Gal staining was restricted to neurons (19, 31).

TABLE 3. Quantification of the number of LAT promoter-positive neurons in TG infected with KOS/1 or 17/1[a]

Virus	Days p.i.	No. of blue neurons/TG pair	
		Mean ± SD	Range
17/1	7	644 ± 101	498–724
KOS/1	7	643 ± 212	348–832
17/1	15	290 ± 144	123–454
KOS/1	15	182 ± 110	89–338
17/1	30	40 ± 8	33–52
KOS/1	30	48 ± 21	21–68

[a] Mice (four per group) were infected with 2×10^6 PFU (total) on both corneas and snouts. At the indicated times, the animals were perfused and the TG were processed for the histochemical detection of β-Gal as described previously (31).

a unique subset of cells. These findings are consistent with the hypothesis that these β-Gal-expressing neurons represent a portion of the latent pool (19, 31).

Frequency of LAT promoter-positive neurons during the acute and latent stages of infection. The LAT promoter–β-Gal reporter mutants 17/1 and KOS/1 were used to examine the relative frequency of latent infections on a cellular level. It is becoming clear that more neurons harbor the latent viral genome than contain LAT RNAs detectable by in situ hybridization (23, 26, 28). In addition, sequences that reside outside the 850-bp basal LAT gene promoter used here may influence expression in neurons during latency (3, 17, 24). However, this promoter is active in a subset of latently infected TG neurons for at least 180 days p.i. (31), and the promoter-reporter transgenes present in 17/1 and KOS/1 are identical in both sequence and context within the viral genome. Therefore, the number of β-Gal-positive neurons present in ganglia infected by these mutants should reflect the relative efficiency of establishment of the two isolates.

Mice were infected as described above, and at 7, 15, and 30 days p.i., TG were harvested and processed for the histochemical detection of β-Gal activity. Whole mounts were coded, and the number of positive cells in each TG pair was determined (Table 3). No statistically significant difference between 17/1 and KOS/1 was seen at any time point analyzed. This result suggests that the numbers of neurons in which latency was established were similar in the two strains.

Frequency of HSV DNA-containing neurons in ganglia latently infected with KOS/M, 17syn+, or McKrae. CXA-D was used to determine the percentage of infected neurons in ganglia latently infected with KOS/M, 17syn+, or McKrae. Mice which had been inoculated via corneal scarification with 1×10^5 to 2×10^5 PFU at least 30 days prior were perfusion fixed, and the TG were dissociated as described above. The neuronal cell populations obtained from six ganglia from each group were analyzed as individual neurons, using the pretreatment procedures and PCR protocol detailed in Materials and Methods. Two sets of six ganglia from the KOS/M and 17syn+ groups were harvested and analyzed. The percentages of neurons infected (PIN) in the two sets of ganglia latent with KOS/M were 29 and 27, not different from the PIN in 17syn+-infected ganglia of 27 and 26 or McKrae of 32 ($P = 0.89$, chi-square test). A diagram of CXA-D and representative panels of the data generated from over 800 PCR samples are shown in Fig. 4. These data demonstrated that the reduced reactivation phenotype characteristic of KOS/M-infected mice could not be explained on the basis of the number of latently infected neurons in the ganglia.

Viral genome copy number within individual neurons. In addition to the number of neurons containing the viral genome, the number of copies of the genome within individual neurons may affect reactivation. Therefore, CXA-D was used to determine the range and mean of the number of viral genome copies within individual neurons comprising the latent pool in KOS/M-, 17syn+-, and McKrae-infected ganglia. The signal intensity from each positive neuron sample was quantified by using ImageQuant software and the copy number determined from a standard curve run with each set of neuron samples. Analysis of the individual positive neurons from each group revealed that the neurons comprising the latent pools of both efficient reactivator strains, 17syn+ and McKrae, contained a greater number of viral genome copies than did KOS/M-infected neurons (Fig. 5). The number of viral genome copies in neurons latently infected with 17syn+ ranged from 1 to 815, with a mean of 50 copies and a median of 14; McKrae-

FIG. 4. Analysis of latent infections at the single-cell level. Latently infected mice were processed for determination of PIN by using CXA-D. (A) Flow diagram of CXA-D. (B) Representative southern blots of the PCR products probed with a [γ-^{32}P]ATP-labeled oligonucleotide internal to the amplification primers. The first four lanes are standards (stds) containing known amounts of HSV-1 DNA, representing the indicated genome equivalents. The fifth lane is a buffer blank performed on cell-free immobilized DNase-treated supernatant from the purified neuron preparations. As expected, the majority of the neurons tested did not contain any viral genomes. The number of neurons positive/the number tested and the PIN are shown on the right.

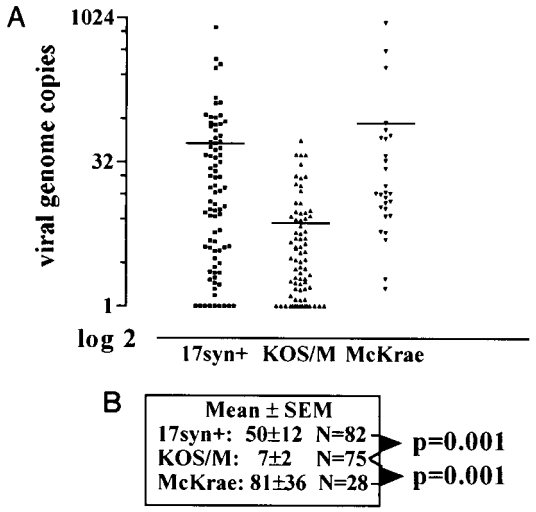

FIG. 5. Analysis of HSV-1 latent genome copy number profiles. The data generated as in Fig. 3 were analyzed on a Molecular Dynamics PhosphorImager using ImageQuant software. The total counts per minute in each band was determined and compared to the values obtained for the standards included with each set of PCRs. (A) Scattergram of the results. Each point represents the number of HSV-1 genomes detected in a single neuron plotted on a semi-$\log_2$ graph to decompress the points. Horizontal bars within the columns mark the mean values. (B) Means ± standard errors. 17syn+ and McKrae groups were not different ($P = 0.287$, unpaired t test). The KOS/M samples were statistically different from both 17syn+ and McKrae ($P = 0.001$, unpaired t test).

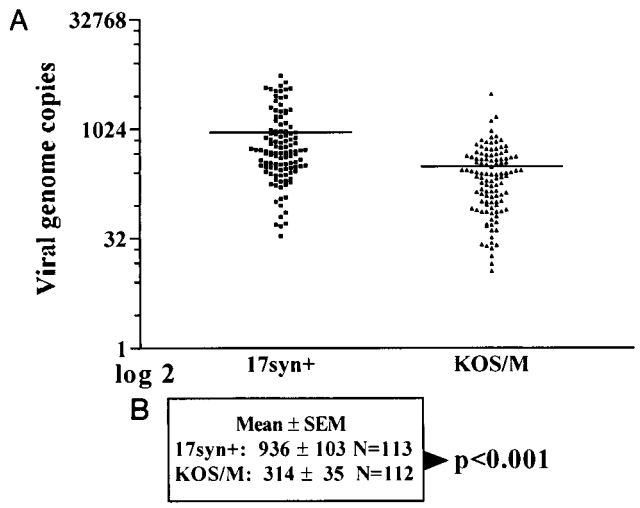

FIG. 6. Analysis of HSV-1 genome copy number profiles in samples of 10 latently infected neurons. The PIN generated in Fig. 3 was used to dilute the purified neurons such that each PCR contained approximately 10 latently infected cells (~40 total neurons). As described in Materials and Methods, the number of PCR cycles was adjusted to maintain linearity in the standard sample between 100 and 10,000 copies. (A) Scattergram of results; (B) means ± standard errors.

infected neurons contained from 1 to 910 copies, with a mean of 82 and a median of 15. The means of these two populations were not different ($P = 0.287$, unpaired t test). The number of viral genome copies in KOS/M-infected neurons ranged from 1 to 53, with a mean of 7 and a median of 3. The mean copy number of the KOS/M latent pool was significantly different from that for both 17syn+ ($P = 0.001$) and McKrae ($P = 0.001$) (Fig. 5). Thus, both of the efficient reactivator strains 17syn+ and McKrae established latent infections containing significantly more viral genome copies than the low-reactivator strain KOS/M.

It was of interest to compare these results with those obtained by QPCR on total ganglia DNA. For strain 17syn+, 26.5% of the neurons harbored the latent genome, and these neurons contained an average of 50 copies of HSV-1. A pair of mouse ganglia contains approximately 40,000 neurons (3, 28). Therefore, $40{,}000 \times 0.265 \times 50 = 5 \times 10^5$ total genomes predicted, and QPCR detected $2.0 \times 10^5 \pm 1.3 \times 10^5$. For KOS/M, $40{,}000 \times 0.279 \times 7 = 7.8 \times 10^4$, and QPCR detected $1.2 \times 10^5 \pm 7.5 \times 10^4$. Although these experiments were performed at different times, the results were quite similar with the different approaches.

Viral genome copy number within groups of latently infected neurons. The analysis of individual neurons is limited in that only a small percentage of neurons in the latent pool can be practically analyzed. Although the prediction would be that those analyzed would reflect the larger population, we developed an assay which provided a view of the copy number in a more extensive portion of the latent pool. This assay was used to confirm our findings at the individual neuron level for 17syn+ and KOS/M. From the PIN, groups of neurons were aliquoted such that each PCR would be predicted to contain 10 HSV-positive neurons. The number of PCR amplification cycles was reduced so that the linear range of the standard curve extended from 100 to 10,000 genomes and differences between 1,000 and 10,000 genomes could now be reproducibly determined. Results of this analysis which included over 1,000 latently infected neurons, or ~1/5 of the total latent pool/ganglion from each group, are shown in Fig. 6. The mean viral genome copy number was 936 in the 17syn+ samples, compared to 314 in the KOS/M group. The means of the two populations were significantly different ($P < 0.0001$, unpaired t test), results consistent with those obtained from the analysis on single cells.

DISCUSSION

Multiple factors may influence the potential of an HSV-1 strain to reactivate from latency. These include functions that dictate the efficient establishment of latency such as replication at the body surface, transport to the ganglionic neurons, and suppression of acute replication within the neurons. Viral functions that are directly linked to reactivation include viral regulatory sequences and gene products that control the initiation of lytic viral gene transcription in response to stress and progression to production of infectious virus. Commonly used HSV-1 laboratory strains differ in the capacity to reactivate from latency. For example, strains 17syn+ and McKrae have been shown to reactivate more efficiently than strain KOS in a variety of systems, including induction by UV light and hyperthermic stress in the mouse and by iontophoresis of epinephrine, immunosuppression, and corneal blebbing with distilled water in the rabbit ocular model (6, 8, 9, 24, 29, 31, 34, 35, 38). In this report, the basis underlying the difference in reactivation in the mouse was explored, focusing on the ability of these strains to establish latent infections.

Three methods were used to measure the establishment of latency. QPCR on total ganglia DNA suggested that there was more latent HSV-1 DNA in ganglia infected by 17syn+ than those infected by KOS/M, but this difference was not significant at the 95% confidence interval. This assay is best suited to detect relatively large differences in DNA content (12). Experiments with the LAT promoter–β-Gal reporter viruses 17/1

and KOS/1 demonstrated that equivalent numbers of neurons expressed the basal LAT promoter at early and late times p.i. Sensitive PCR-based methods have demonstrated that these β-Gal-positive cells must represent only a subset of those that harbor the latent viral genome (18, 26, 28, 38). The assumption was made that these cells represent the same fraction of latently infected neurons in the background of either strain, but this may not be the case. For example, the difference in the number of HSV-1 genomes present in individual neurons latently infected with 17syn+ and KOS/M reported here could effect the level of LAT promoter activity. The CXA-D approach allowed the direct determination of the percentage of neurons within latently infected ganglia that harbor the viral genome. This assay is sensitive enough to detect one or a very few HSV-1 genome copies within individual neurons (28, 38). Interestingly, the number of neurons latently infected in the TG was not different for 17syn+, McKrae, or KOS/M. However, the number of viral genome copies constituting each latent infection was significantly greater in 17syn+- and McKrae-infected neurons than in KOS/M-infected neurons. This three- to sevenfold increase in latent genome copy number was consistent with the increased total latent DNA detected in 17syn+-infected TG compared to that of KOS/M-infected TG.

The biological significance of this difference is not yet clear. We hypothesize that the higher copy number of latent viral genomes present in neurons latently infected with strains 17syn+ or McKrae contributes to the ability of these strains to reactivate efficiently in vivo. Several possible mechanisms whereby viral genome copy number might influence reactivation from the latent state can be envisioned. Many viral genome copies could effectively overwhelm factors silencing viral gene transcription, leading to an increased probability of reactivation. Alternatively or additionally, the increased number of viral gene templates available for transcription during the initiation of reactivation may result in increased production of viral proteins required for successful entry into the lytic cascade as hypothesized by Sears and Roizman (33). Kosz-Vnenchak et al. proposed a variation of this hypothesis which included the requirement for replication of the viral genome prior to sufficient immediate-early gene transcription (13, 14). However, until recently, viral genome copy number had not been measured in individual neurons (28). The fact the viral genome copy number set point varies among viral strains and correlates with reactivation competency is the first experimental data to support the hypothesis that copy number may be a controlling factor for reactivation.

A central question is the origin of the multiple copies of the HSV-1 genome within individual latently infected neurons. Sears and Roizman have speculated that the genome may replicate during latency, utilizing as yet undefined neuronal mechanisms and a putative eukaryotic replication origin found within the viral genome (33). Such a mechanism might be operative and important for replenishing the pool of high-copy-number (i.e., reactivatable) neurons over the life of the host. The simplest explanation is that they arise during the acute infection phase as a result of either multiple infection of single neurons or limited genome replication within neurons and their subsequent entry into the latent state. Of these, we favor the first possibility for the following reasons. First, it is generally recognized that lytic infection progressing through viral DNA replication is fatal to the host cell (5). Thus, an as yet unknown mechanism to ensure the survival of neurons in vivo would have to be operative. Infection of a single neuron by multiple virions that enter the latent state does not require conjecture of any additional altered replication pathways. Reinfection of cells in culture is inhibited by expression of gD on the infected cell surface (27). However, it is unlikely that such a potent target for immune attack is expressed on the surface of neurons in which latency is established. Second, infection of mice on the snout with a genetically engineered TK-negative mutant resulted in efficient replication at the surface but extremely limited replication within the TG. The viral genome copy number in the latent pool of neurons in these mice was not significantly different from that for the wt or the rescue, suggesting that it is replication at the surface and not within the TG that is important for this phenomenon (32).

There have been several studies comparing viral strains with different abilities to reactivate. Strelow et al. (34) compared strains KOS and McKrae with the UV induction model in the mouse eye. McKrae reactivated efficiently, whereas the reactivation of KOS was inefficient. A recombinant virus in which the LAT promoter and 5′ end of the LAT gene from McKrae were used to replace the highly homologous sequences present in strain KOS failed to reactivate, suggesting that these sequences were not sufficient to donate the frequent reactivation phenotype to KOS (34). Gordon et al. (6) investigated the establishment of latency of frequent and low-reactivation strains in the rabbit eye model. In situ hybridization for the LAT RNAs was used to quantify latent infections; by this measure, rabbit TG latently infected with strain KOS contained very few positive neurons compared to the high-reactivation strain W (6). These data indicated that the number of latent infections was different. The low frequency of LAT-positive neurons detected by Gordon et al. may be due to differences between the rabbit and mouse systems or to altered characteristics of the KOS isolates used. Since a comparison of the acute replication of the strains was not reported, it is not clear how the two strains compared with respect to this important parameter. However, a study by Stroop and Banks demonstrated that an isolate of KOS termed KOS-63 replicated poorly in the rabbit eye and failed to reactivate (35). The KOS isolate used in this study, KOS/M, is different from KOS-63 in that, as reported here, it replicates as efficiently as 17syn+ on the mouse cornea and snout and in the TG. Therefore, in contrast to KOS-63, the reduced capacity of strain KOS/M to reactivate in vivo following hyperthermic stress could not be attributed to any measurable difference in replication competency.

Although we have determined a difference in one characteristic of the latent infections established by KOS/M and two efficient reactivator strains, 17syn+ and McKrae, other viral processes may be involved. Clearly, strain KOS can reactivate, as it does so efficiently in explant cocultivation cultures (2, 10, 16). However, the signals transduced in the neurons by axotomy and culture in vitro may be quite different from those in an intact neuron stressed in vivo. It is possible that strain KOS/M does not initiate reactivation efficiently in vivo in response to stress. The immune response is also absent in vitro, and KOS/M may not progress to production of detectable levels of infectious virus before the reactivating neurons are destroyed. This latter possibility seems less likely since KOS/M replicates efficiently in mouse TG during acute infection (29, 31, 38). However, KOS/M is less neuroinvasive than strain 17 syn+ (37), and this has been mapped at least in part to a mutation in gB that may result in a heightened immune response against this strain (10). Further confirmation of the potential role of the latent genome copy profile and reactivation will come from the manipulation of infection strategies to alter the copy number profile of a given HSV-1 strain. This will allow the determination of the effect on reactivation in the absence of complications arising from genetic variance among

virus strains. An analysis of the molecular basis for differences in latent infections established by various isolates will yield new insights into the viral factors that regulate the establishment and reactivation of HSV latent infections.

ACKNOWLEDGMENTS

This work was supported by Public Health Service grants AI32121 from the National Institutes of Allergy and Infectious Diseases and NS25879 from the National Institutes of Neurological Communicative Disorders and Stroke and by CHMCC Trustee Grant 31-358-639.

REFERENCES

1. **Bloom, D. C., J. M. Hill, G. Devi-Rao, E. K. Wagner, L. T. Feldman, and J. G. Stevens.** 1996. A 348-base-pair region in the latency-associated transcript facilitates herpes simplex virus type 1 reactivation. J. Virol. **70:**2449–2459.
2. **Cai, W., T. L. Astor, L. M. Liptak, C. Cho, D. M. Coen, and P. A. Schaffer.** 1993. The herpes simplex virus type 1 regulatory protein ICP0 enhances virus replication during acute infection and reactivation from latency. J. Virol. **67:**7501–7512.
3. **Davies, A., and A. Lumsden.** 1984. Relation of target encounter and neuronal death to nerve growth factor responsiveness in the developing mouse trigeminal ganglion. J. Comp. Neurol. **223:**124–137.
4. **Dobson, A. T., T. P. Margolis, W. A. Gomes, and L. T. Feldman.** 1995. In vivo deletion analysis of the herpes simplex virus type 1 latency-associated transcript promoter. J. Virol. **69:**2264–2270.
5. **Glorioso, J. C., N. A. DeLuca, and D. J. Fink.** 1995. Development and application of herpes simplex virus vectors for human gene therapy. Annu. Rev. Microbiol. **49:**675–710.
6. **Gordon, Y. J., E. G. Romanowski, T. Araullo-Cruz, and P. R. Kinchington.** 1995. The proportion of trigeminal ganglionic neurons expressing herpes simplex virus type 1 latency-associated transcripts correlates to reactivation in the New Zealand rabbit ocular model. Graefe's Arch. Clin. Exp. Ophthalmol. **233:**649–654.
7. **Herold, B. C., D. WuDunn, N. Soltys, and P. G. Spear.** 1991. Glycoprotein C of herpes simplex virus type 1 plays a principal role in the adsorption of virus to cells and in infectivity. J. Virol. **65:**1090–1098.
8. **Hill, J. M., H. H. Garza, Jr., Y. H. Su, R. Meegalla, L. A. Hanna, J. M. Loutsch, H. W. Thompson, E. D. Varnell, D. C. Bloom, and T. M. Block.** 1997. A 437-base-pair deletion at the beginning of the latency-associated transcript promoter significantly reduced adrenergically induced herpes simplex virus type 1 ocular reactivation in latently infected rabbits. J. Virol. **71:**6555–6559.
9. **Hill, J. M., J. B. Maggioncalda, H. H. Garza, Jr., Y. H. Su, N. W. Fraser, and T. M. Block.** 1996. In vivo epinephrine reactivation of ocular herpes simplex virus type 1 in the rabbit is correlated to a 370-base-pair region located between the promoter and the 5′ end of the 2.0-kilobase latency-associated transcript. J. Virol. **70:**7270–7274.
10. **Izumi, K. M., and J. G. Stevens.** 1990. Molecular and biological characterization of a herpes simplex virus type 1 (HSV-1) neuroinvasiveness gene. J. Exp. Med. **172:**487–496.
11. **Jacobson, J. G., K. L. Ruffner, M. Kosz-Vnenchak, C. B. Hwang, K. K. Wobbe, D. M. Knipe, and D. M. Coen.** 1993. Herpes simplex virus thymidine kinase and specific stages of latency in murine trigeminal ganglia. J. Virol. **67:**6903–6908.
12. **Katz, J. P., E. T. Bodin, and D. M. Coen.** 1990. Quantitative polymerase chain reaction analysis of herpes simplex virus DNA in ganglia of mice infected with replication-incompetent mutants. J. Virol. **64:**4288–4295.
13. **Kosz-Vnenchak, M., D. M. Coen, and D. M. Knipe.** 1990. Restricted expression of herpes simplex virus lytic genes during establishment of latent infection by thymidine kinase-negative mutant viruses. J. Virol. **64:**5396–5402.
14. **Kosz-Vnenchak, M., J. Jacobson, D. M. Coen, and D. M. Knipe.** 1993. Evidence for a novel regulatory pathway for herpes simplex virus gene expression in trigeminal ganglion neurons. J. Virol. **67:**5383–5393.
15. **Kramer, M. F., and D. M. Coen.** 1995. Quantification of transcripts from the ICP4 and thymidine kinase genes in mouse ganglia latently infected with herpes simplex virus. J. Virol. **69:**1389–1399.
16. **Leib, D. A., D. M. Coen, C. L. Bogard, K. A. Hicks, D. R. Yager, D. M. Knipe, K. L. Tyler, and P. A. Schaffer.** 1989. Immediate-early regulatory gene mutants define different stages in the establishment and reactivation of herpes simplex virus latency. J. Virol. **63:**759–768.
17. **Lokensgard, J. R., H. Berthomme, and L. T. Feldman.** 1997. The latency-associated promoter of herpes simplex virus type 1 requires a region downstream of the transcription start site for long-term expression during latency. J. Virol. **71:**6714–6719.
18. **Maggioncalda, J., A. Mehta, Y. H. Su, N. W. Fraser, and T. M. Block.** 1996. Correlation between herpes simplex virus type 1 rate of reactivation from latent infection and the number of infected neurons in trigeminal ganglia. Virology **225:**72–81.
19. **Margolis, T. P., D. C. Bloom, A. T. Dobson, L. T. Feldman, and J. G. Stevens.** 1993. Decreased reporter gene expression during latent infection with HSV LAT promoter constructs. Virology **197:**585–592.
20. **McGeoch, D. J., C. Cunningham, G. Mcintyre, and A. Dolan.** 1991. Comparative sequence analysis of the long repeat regions and adjoining parts of the long unique regions in the genomes of herpes simplex viruses type-1 and type-2. J. Gen. Virol. **72:**3057–3075.
21. **McGeoch, D. J., M. A. Dalrymple, A. J. Davison, A. Dolan, M. C. Frame, D. McNab, L. J. Perry, J. E. Scott, and P. Taylor.** 1988. The complete DNA sequence of the long unique region in the genome of herpes simplex virus type 1. J. Gen. Virol. **69:**1531–1574.
22. **McGeoch, D. J., A. Dolan, S. Donald, and F. J. Rixon.** 1985. Sequence determination and genetic content of the short unique region in the genome of herpes simplex virus type 1. J. Mol. Biol. **181:**1–13.
23. **Mehta, A., J. Maggioncalda, O. Bagasra, S. Thikkavarapu, P. Saikumari, T. Valyi-Nagy, N. W. Fraser, and T. M. Block.** 1995. In situ DNA PCR and RNA hybridization detection of herpes simplex virus sequences in trigeminal ganglia of latently infected mice. Virology **206:**633–640.
24. **Perng, G. C., K. Chokephaibulkit, R. L. Thompson, N. M. Sawtell, S. M. Slanina, H. Ghiasi, A. B. Nesburn, and S. L. Wechsler.** 1996. The region of the herpes simplex virus type 1 LAT gene that is colinear with the ICP34.5 gene is not involved in spontaneous reactivation. J. Virol. **70:**282–291.
25. **Rader, K. A., C. E. Ackland-Berglund, J. K. Miller, J. S. Pepose, and D. A. Leib.** 1993. In vivo characterization of site-directed mutations in the promoter of the herpes simplex virus type 1 latency-associated transcripts. J. Gen. Virol. **74:**1859–1869.
26. **Ramakrishnan, R., M. Levine, and D. J. Fink.** 1994. PCR-based analysis of herpes simplex virus type 1 latency in the rat trigeminal ganglion established with a ribonucleotide reductase-deficient mutant. J. Virol. **68:**7083–7091.
27. **Roller, R. J., and B. Roizman.** 1994. A herpes simplex virus 1 US11-expressing cell line is resistant to herpes simplex virus infection at a step in viral entry mediated by glycoprotein D. J. Virol. **68:**2830–2839.
28. **Sawtell, N. M.** 1997. Comprehensive quantification of herpes simplex virus latency at the single-cell level. J. Virol. **71:**5423–5431.
29. **Sawtell, N. M., and J. L. Lessard.** 1989. Cellular distribution of smooth muscle actins during mammalian embryogenesis: expression of the a-vascular but not the g-enteric isoform in differentiated striated myocytes. J. Cell Biol. **109:**2929–2937.
30. **Sawtell, N. M., and R. L. Thompson.** 1992. Rapid in vivo reactivation of herpes simplex virus in latently infected murine ganglionic neurons after transient hyperthermia. J. Virol. **66:**2150–2156.
31. **Sawtell, N. M., and R. L. Thompson.** 1992. Herpes simplex virus type 1 latency-associated transcription unit promotes anatomical site-dependent establishment and reactivation from latency. J. Virol. **66:**2157–2169.
32. **Sawtell, N. M., and R. L. Thompson.** Unpublished data.
33. **Sears, A., and E. B. Roizman.** 1990. Amplification by host cell factors of a sequence contained within the herpes simplex virus 1 genome. Proc. Natl. Acad. Sci. USA **87:**9441–9444.
34. **Strelow, L. I., K. A. Laycock, P. Y. Jun, K. A. Rader, R. H. Brady, J. K. Miller, J. S. Pepose, and D. A. Leib.** 1994. A structural and functional comparison of the latency-associated transcript promoters of herpes simplex virus type 1 strains KOS and McKrae. J. Gen. Virol. **75:**2475–2480.
35. **Stroop, W. G., and M. C. Banks.** 1994. Herpes simplex virus type 1 strain KOS-63 does not cause acute or recurrent ocular disease and does not reactivate ganglionic latency in vivo. Acta Neuropathol. (Berlin) **87:**14–22.
36. **Tenser, R. B.** 1991. Role of herpes simplex virus thymidine kinase expression in viral pathogenesis and latency. Intervirology **32:**76–92.
37. **Thompson, R. L., M. L. Cook, G. Devi-Rao, E. K. Wagner, and J. G. Stevens.** 1986. Functional and molecular analysis of the avirulent wild-type herpes simplex virus type 1 strain KOS. J. Virol. **58:**203–211.
38. **Thompson, R. L., and N. M. Sawtell.** 1997. The herpes simplex virus type 1 latency-associated transcript gene regulates the establishment of latency. J. Virol. **71:**5432–5440.
39. **Thompson, R. L., and J. G. Stevens.** 1983. Biological characterization of a herpes simplex virus intertypic recombinant which is completely and specifically non-neurovirulent. Virology **131:**171–179.
40. **Thompson, R. L., E. K. Wagner, and J. G. Stevens.** 1983. Physical location of a herpes simplex virus type 1 gene function(s) specifically associated with a 10 million-fold increase in HSV neurovirulence. Virology **131:**180–192.